JOURNAL OF GUIDANCE, CONTROL, AND DYNAMICS
Vol. 15, No. 5, September-October 1992

Active Vibration Absorber for the CSI Evolutionary Model: Design and Experimental Results

Anne M. Bruner*
Lockheed Engineering & Sciences Company, Hampton, Virginia 23666
and
W. Keith Belvin,† Lucas G. Horta,‡ and Jer-Nan Juang§
NASA Langley Research Center, Hampton, Virginia 23665

The development of control technology for large flexible structures must include practical demonstrations to aid in the understanding of controlled structures in space. To support this effort, a testbed facility has been developed to study practical implementation of new control technologies. The paper discusses the design of a second-order acceleration feedback controller that acts as an active vibration absorber. This controller provides guaranteed stability margins for collocated accelerometer/actuator pairs in the absence of accelerometer/actuator dynamics and computational time delay. Experimental results in the presence of these factors are presented and discussed. The primary performance objective considered is damping augmentation of the first nine structural modes. Comparison of experimental and predicted closed-loop damping is presented, including test and simulated-time histories for open- and closed-loop cases. Although the simulation and test results are not in full agreement, robustness of this design under model uncertainty is demonstrated. The basic advantage of this second-order controller design is that the stability of the controller is model-independent for collocated accelerometers and actuators.

Introduction

LARGE space structure control requires special control design methodologies. High modal density in the controller bandwidth makes rolloff of control authority a problem. Many of the theoretical issues with regard to large space structure control were recognized and initially treated by Ref. 1. Experimental validation is now being demonstrated with a series of facilities that have been designed for that purpose.[2-4] It is recognized that the complexity of these structures foster the use of controllers with high and low authority. Theoretically, low-authority controllers are used to augment the inherent damping of the structure, while the high-authority controllers are designed to achieve the desired performance. One form of these low-authority controllers is an active vibration absorber, which is the subject of this paper.

NASA has undertaken a Controls Structure Interaction (CSI) program for the design, development, and fabrication of generic structures to study fundamental problems in the implementation of advanced control methodologies. The program stresses the application of existing sensor and actuator technologies for identification and control. An early testbed of the CSI program has been completed at the NASA Langley Research Center. The configuration selected, which is described in detail in a later section, uses thrusters and accelerometers as its primary actuation and sensing devices. Initially, controller designs that would not require knowledge of the dynamics of the structure are preferred. This allows the implementation of such controllers even when model uncertainties are large. For this purpose, a procedure for designing second-order controllers using positivity concepts is discussed for continuous time systems.[5] Using this approach, decentralized controllers have been designed and used for experimental validation.

The paper outline is as follows. First the controller design theory is presented followed by a mechanical analogy. A brief description of the testbed is given, and a controller design procedure for the laboratory model is described. Finally, test results from the experimental implementation are provided and compared with the analytical results.

Controller Design Theory

For large scale systems, a model of the structure is often obtained via finite element methods resulting in a second-order differential equation of the form.

$$M\ddot{x} + D\dot{x} + Kx = Bu \tag{1}$$

Here x is an $n \times 1$ displacement vector, and M, D, and K are mass, damping, and stiffness matrices, respectively, which generally are symmetric and sparse. The $n \times p$ influence matrix B describes the actuator force distributions for the $p \times 1$ input vector u. In this paper, only acceleration measurements are assumed available and this leads to a plant output equation of the form

$$y = H_a\ddot{x} \tag{2}$$

where y is an $m \times 1$ measurement vector and H_a the $m \times n$ acceleration influence matrix. For direct output feedback control, the input vector u can be written

$$u = -Gy = -GH_a\ddot{x} \tag{3}$$

where G is a gain matrix to be determined. Substituting Eq. (3) into Eq. (1) yields

$$(M + BGH_a)\ddot{x} + D\dot{x} + Kx = 0 \tag{4}$$

Received March 15, 1991; revision received Oct. 28, 1991; accepted for publication Nov. 12, 1991.

*Structural Control Engineer.
†Aerospace Engineer, Spacecraft Dynamics Branch. Senior Member AIAA.
‡Aerospace Engineer, Spacecraft Dynamics Branch. Member AIAA.
§Principal Scientist, Spacecraft Dynamics Branch. Associate Fellow AIAA.

Equation (4) shows that damping cannot be directly augmented with direct output feedback unless additional dynamics are introduced.

Let a controller be designed to have a set of second-order dynamic equations and measurement equations similar to the system equations, Eqs. (1) and (2):

$$M_c\ddot{x}_c + D_c\dot{x}_c + K_c x_c = B_c u_c \tag{5}$$

$$y_c = H_{ac}\ddot{x}_c \tag{6}$$

Here x_c is the controller coordinate of dimension n_c, and M_c, D_c, and K_c can be interpreted as the controller mass, damping, and stiffness matrices, respectively, which in general are symmetric and positive definite to make the controller asymptotically stable. The $n_c \times m$ matrix B_c describes the input distributions for the $m \times 1$ vector u_c. Equation (6) is the controller output equation having y_c as the output vector of length p and H_{ac} a $p \times n_c$ acceleration influence matrix. The quantities u_c, y_c, and n_c are arbitrary, which means that M_c, D_c, K_c, H_{ac}, and B_c are the design parameters for the controller.

Let the input vector u in Eq. (1) and Eq. (5) be

$$u = y_c = H_{ac}\ddot{x}_c \tag{7}$$

$$u_c = y = H_a\ddot{x} \tag{8}$$

Substituting Eq. (7) into Eq. (1) and Eq. (8) into Eq. (5) yields

$$M_t\ddot{x}_t + D_t\dot{x}_t + K_t x_t = 0 \tag{9}$$

where

$$M_t = \begin{bmatrix} M & -BH_{ac} \\ -B_c H_a & M_c \end{bmatrix}, \qquad D_t = \begin{bmatrix} D & 0 \\ 0 & D_c \end{bmatrix}$$

$$K_t = \begin{bmatrix} K & 0 \\ 0 & K_c \end{bmatrix}, \qquad x_t = \begin{Bmatrix} x \\ x_c \end{Bmatrix}$$

If the design parameters are chosen such that M_t, D_t, and K_t are positive definite, the closed-loop system, Eq. (9), becomes asymptotically stable.

For M_t to be a real positive definite matrix, it must satisfy

$$x_t^T M_t x_t > 0 \tag{10}$$

for any real vector x_t except the null vector. If M_t is to be symmetric, it is required that

$$BH_{ac} = H_a^T B_c^T \tag{11}$$

For collocated sensors and actuators,

$$B = H_a^T \tag{12}$$

so that it is only required that

$$H_{ac} = B_c^T \tag{13}$$

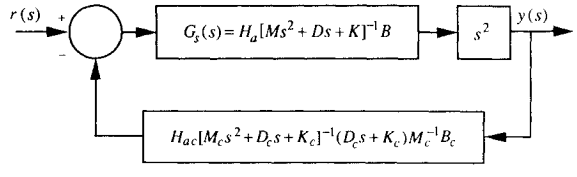

Fig. 1 Block diagram of closed-loop system with general acceleration feedback.

Substituting the definition of x_t and M_t into Eq. (10) and using the symmetry condition of Eq. (11) yields

$$x_t^T M_t x_t = x^T(M - BH_{ac}H_{ac}^T B^T)x + (H_{ac}^T B^T x - x_c)^T(H_{ac}^T B^T x - x_c) + x_c^T(M_c - I)x_c$$

This equation is greater than zero if H_{ac} and M_c are chosen such that $M - BH_{ac}H_{ac}^T B^T$ and $M_c - I$ are positive definite. Note that these are sufficient, but not necessary conditions.

To obtain a controller structure without this restriction on H_{ac} and M_c, let the u in Eq. (7) be modified to include a direct acceleration feedback term. Then

$$u = y_c - G_a y = H_{ac}\ddot{x}_c - G_a y \tag{14}$$

which makes

$$M_t = \begin{bmatrix} M + BG_a H_a & -BH_{ac} \\ -B_c H_a & M_c \end{bmatrix} \tag{15}$$

Defining

$$G_a = H_{ac}M_c^{-1}B_c \tag{16}$$

substituting into Eq. (15), and using the symmetry condition in Eq. (11), the positive definite condition in Eq. (10) becomes

$$x_t^T M_t x_t = x^T M x + (M_c^{-1}B_c H_a x - x_c)^T M_c(M_c^{-1}B_c H_a x - x_c) \tag{17}$$

which is positive if M and M_c are positive definitive matrices. Figure 1 shows a block diagram of the closed-loop system with acceleration feedback.

In this section, it has been proven that a second-order controller can be designed for any collocated plant that can be expressed in terms of Eqs. (1) and (2) and the stability of the closed-loop system is model-independent. The controller is described by

$$M_c\ddot{x}_c + D_c\dot{x}_c + K_c x_c = B_c u_c = B_c y \tag{18}$$

$$u = y_c - G_a y = H_{ac}\ddot{x}_c - H_{ac}M_c^{-1}B_c y \tag{19}$$

Sufficient conditions for closed-loop stability are that M_c, D_c, and K_c be positive and that $H_{ac} = B_c^T$.

Vibration Absorber Analogy

The second-order controller structure can be thought of as attaching an additional mass, spring, and damper assembly to the structure at the location of the sensors/actuators. For the case of a single mode plant, a diagram representing the closed-loop system is shown in Fig. 2. Letting $x_c = x_a - x$ results in plant and controller equations:

Plant:

$$m\ddot{x} + d\dot{x} + kx = bu$$

$$y = h_a\ddot{x} \tag{20}$$

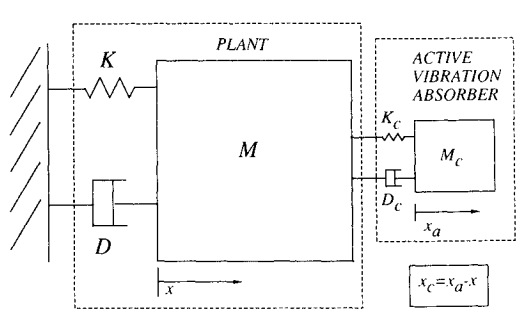

Fig. 2 Single mode structure controller design model.

Controller:

$$m_c\ddot{x}_c + d_c\dot{x}_c + k_c x_c = -m_c y$$

$$u = k_c x_c + d_c \dot{x}_c \tag{21}$$

A block diagram for this physical system is shown in Fig. 3. Upon comparison of Fig. 1 and Fig. 3 (where the matrices in Fig. 1 are now scalars), h_{ac} and b_c must satisfy

$$h_{ac} b_c = m_c^2 \tag{22}$$

Assuming collocated sensors and actuators, the constraints given in Eqs. (13) and (22) yield

$$h_{ac} = -m_c \tag{23}$$

$$b_c = -m_c \tag{24}$$

Using the controller equations given in Eq. (21), a state-space model can be written:

$$\dot{\tilde{x}} = A\tilde{x} + By \tag{25}$$

$$u = C\tilde{x} + Dy \tag{26}$$

where

$$A = \begin{bmatrix} 0 & 1 \\ -k_c/m_c & -d_c/m_c \end{bmatrix}, \qquad B = \begin{bmatrix} 0 \\ -1 \end{bmatrix}$$

$$C = [k_c \;\; d_c], \qquad D = [0], \qquad \tilde{x} = \begin{Bmatrix} x_c \\ \dot{x}_c \end{Bmatrix}$$

The theory described in the previous section shows that for stability of a collocated MIMO system, sufficient conditions on the controller parameters are that M_c, D_c, and K_c be positive definite and that $H_{ac} = B_c^T$. In this paper, the controller is obtained by designing SISO controllers to augment damping in a single mode. To design a SISO controller, a target mode and an input/output pair are selected. The plant is then assumed to be a single mode system, which can be described by

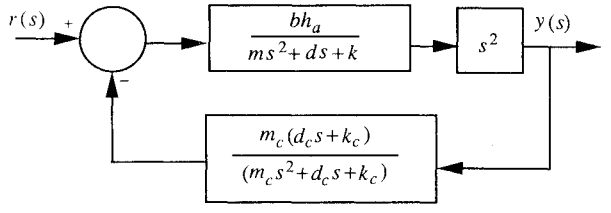

Fig. 3 Block diagram of single mode structure controller closed-loop system.

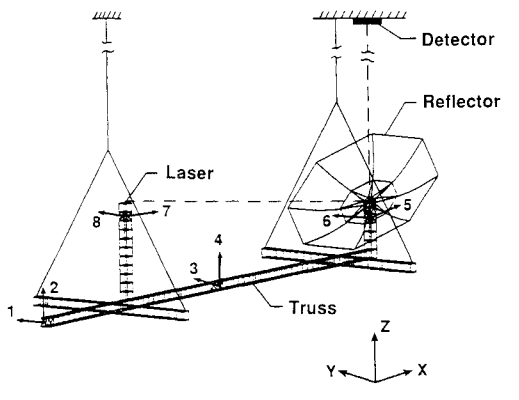

Fig. 4 Schematic of the CSI evolutionary model showing actuator and sensor locations.

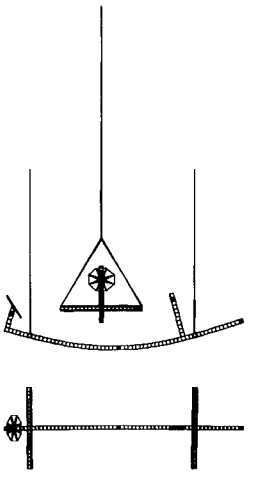

Fig. 5 Vibration mode shape 8 ($f = 1.71$ Hz).

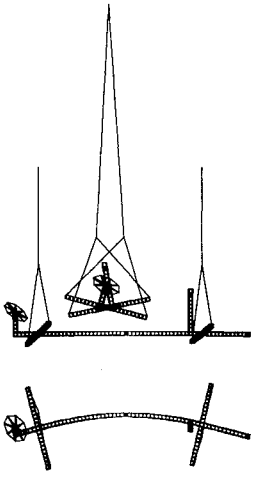

Fig. 6 Vibration mode shape 9 ($f = 1.90$ Hz).

the scalar equations given in Eq. (20) and the SISO controller is defined by Eq. (21). For each of the SISO controllers, m_c, d_c, and k_c are chosen greater than zero and $h_{ac} = b_c = -m_c$. These SISO controllers are then arranged into block diagonal A, B, C, and D matrices given in Eqs. (25) and (26) for implementation.

The low-frequency [$\omega \ll (\sqrt{k_c/m_c})^{1/2}$] gain of the SISO controller equals m_c. In the presence of sensor bias, a large m_c could result in large actuator command offsets or even saturation. It is important to select small values for m_c to reduce the effects of offsets. In analogy with vibration absorbers,[6] the frequency of the absorber is set equal to the targeted mode, i.e., $\omega^2 = k_c/m_c$. After selecting values for m_c and k_c, values for d_c are selected based on root locus design.

Experimental Validation

Laboratory Model Description

The evolutionary model testbed[4] weighs 741 lb and is supported from the ceiling with two steel cables of length 64.5 ft each. The truss is made of aluminum struts forming 10 in cubical bays of single lace diagonals alternating so that opposite faces cross. The major components of the structure are the center section 52.5 ft long, a 16-ft-diameter reflector, and a 9.2-ft tower where a laser beam is located. A total of eight actuator pairs are placed at four locations along the truss as shown in Fig. 4, and each actuator pair is capable of producing 4.4 lbf. In addition, eight accelerometers are collocated with the thrusters for identification and control experiments. The finite element model has 86 modes below 50 Hz. Because of the suspension, the first six structural modes are pendulum

modes with frequencies between 0.1 Hz and 0.9 Hz. The next three modes are bending modes with frequencies between 1.4 Hz and 1.9 Hz. Orthogonal views of the mode shapes for modes 8 and 9 are provided in Figs. 5 and 6. Control laws are implemented on a digital computer at sampling rates of 80 Hz and 350 Hz.

Controller Parameter Selection

The design theory discussed is now used to develop SISO controllers for each actuator/sensor pair.The design approach is to determine the most controllable/observable mode(s) for a particular input/output pair and tune a second-order controller to the mode(s). Each second-order controller has three design parameters, namely, m_c, d_c, and k_c. If one actuator/sensor pair is to control n separated modes, n distinct sets of design parameters need to be determined. The procedure used to design controllers for the evolutionary model is the following:

1) Choose m_c to avoid large command offsets.

2) Choose a target mode for each actuator/sensor pair and determine the value of k_c needed to match its frequency, where $k_c/m_c = \omega^2$.

3) Determine the value of d_c that optimizes the damping value of the target mode.

The design objective is to increase damping in the first nine modes. A value of 0.1 is selected for m_c based on previous experimental results. Note that m_c represents the controller mass coupled to a modal structure, thus, $m_c = 0.1$ is 10% of the generalized mass assuming orthonormalization of the eigenvectors. Each input/output pair was then assigned one or two target modes to control, which determined the value for k_c. To optimize damping, a root locus is performed for each actuator/sensor pair by fixing m_c and k_c and varying d_c. In

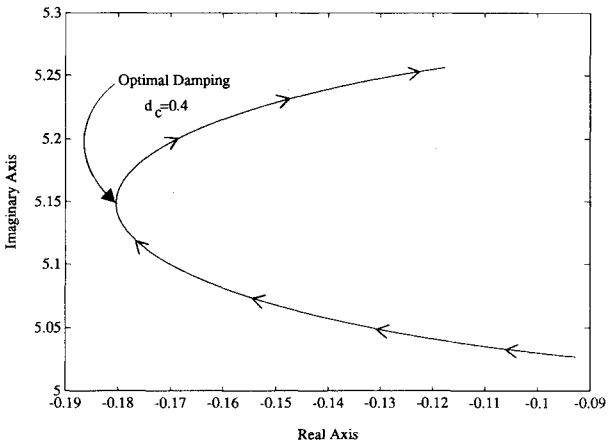

Fig. 7 Mode 6 root locus with controller parameter d_c.

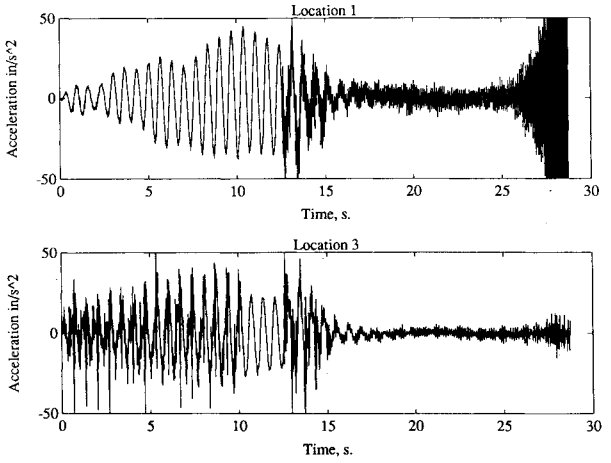

Fig. 8 Unstable closed-loop response at locations 1 and 3.

Table 1 Controller design parameters

	First target mode				Second target mode			
Location	Mode	m_c	d_c	k_c	Mode	m_c	d_c	k_c
1	3	0.1	0.06	0.089	9	0.1	0.4	13.22
2	4	0.1	0.2	2.10	8	0.1	0.5	10.88
3	2	0.1	0.04	0.083	9	0.1	0.4	13.22
4	8	0.1	0.4	10.88	—	—	—	—
5	1	0.1	0.03	0.083	—	—	—	—
6	3	0.1	0.04	0.083	—	—	—	—
7	1	0.1	0.03	0.083	8	0.1	0.4	10.88
8	6	0.1	0.4	3.95	—	—	—	—

locations where more than one controller is used, each controller is optimized separately. Figure 7 shows the root locus for mode 6 using actuator/sensor pair 8 for values of d_c ranging from 0.1 to 1.0. A maximum damping value of 3.5% is achieved when $d_c = 0.4$. The modes selected, the corresponding actuator/sensor pair used to control them, and control design parameters are presented in Table 1.

Implementation Issues

The controllers described in the previous section have special properties that must be considered in the actual implementation. The implementation of the active vibration absorber (AVA) controller should ideally emulate a physical spring-mass-damper attached to a structure at a single point. Time response data from the initial implementation of the controller described in the previous section is given in Fig. 8. In this experiment, the structure was excited for 10 s in two pendulum modes and two bending modes, allowed to free decay for 3 s, and then the controller was turned on at 13 s. The closed-loop system is unstable at a mode around 7 Hz.

In the theoretical portion of this paper, it was stated that this controller is guaranteed stable provided that m_c, d_c, and k_c are chosen positive and Eq. (11) is satisfied. By referencing Table 1 for the controller design parameters, all values for m_c, d_c, and k_c are positive, which leaves us with Eq. (11). By setting h_{ac} and b_c equal to $-m_c$ as in Eqs. (23) and (24), an assumption of collocation was made. Sensor and actuator collocation must be spatial and temporal. Spatial collocation implies that the sensor and actuator are located at the exact same location on the structure. Typical mounting of sensors and actuators result in spatially close arrangements, not collocated. Temporal collocation is satisfied when there is no phase shift due to sensor/actuator dynamics or due to digital implementation of the control law. Hence, temporal collocation can be most closely achieved with very large bandwidth sensors and actuators and analog computations.

After the initial implementation of the AVA controller, an attempt was made to improve both the spatial and temporal collocation of the closed-loop system. The implementation was improved by 1) improving the spatial collocation of sensors and actuators; 2) optimizing the software to increase the sampling frequency; and c) resequencing the controller computational steps to reduce time delay.This is possible because the AVA controller is not an observer-based controller. Hence, the use of acceleration measurements does not require a direct transmission term, (i.e., $D = 0$).

Once these improvements were made, the same AVA controller was once again implemented on the testbed. The time history plots are presented in Fig 9.

Simulation and Test Comparison

In determining the success of the AVA controller, each of the nine modes was excited independently, and the controller was then activated for vibration suppression. The top of Fig. 10 shows the experimental open- and closed-loop accelerometer responses dominated by the eighth mode of the structure. For open loop, the structure is excited using sinusoidal excitation at the frequency of the mode of interest for 10 cycles. For

Table 2 Comparison of experimental and analytical frequency and damping results

	Frequency, Hz		Damping, %		
Mode	Experimental	Analysis	Experimental Open loop	Experimental Closed loop	Analysis Closed loop
1	0.145	0.147	5.7	10.6	9.4
2	0.149	0.149	7.5	7.5	11.3
3	0.148	0.155	7.5	13.5	13.0
4	0.718	0.730	0.7	8.2	6.0
5	0.740	0.748	0.7	6.2	0.8
6	0.900	0.874	0.2	4.7	3.3
7	1.500	1.474	0.2	9.3	4.3
8	1.710	1.738	0.3	13.1	12.5
9	1.900	1.883	0.3	8.0	5.2

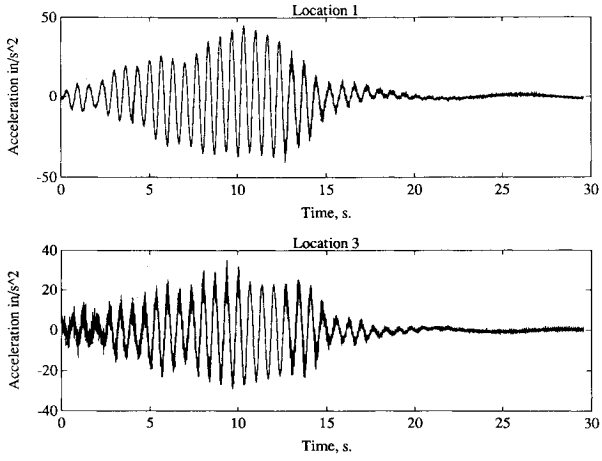

Fig. 9 Stable closed-loop response at locations 1 and 3.

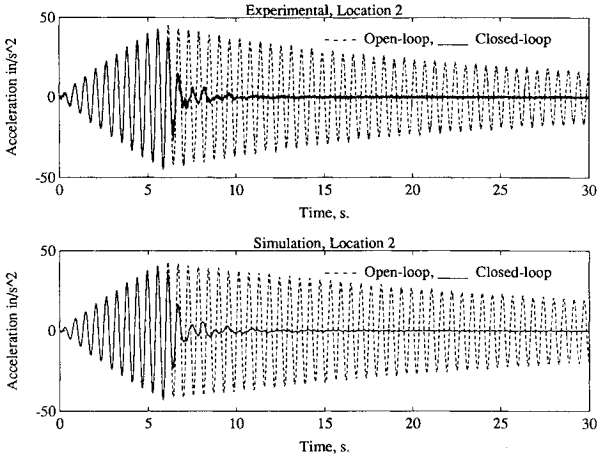

Fig. 10 Open- and closed-loop responses at location 2.

closed loop, the structure is excited in the same manner, and then the controller is activated for the duration of each test. Shown in the bottom of Fig. 10 are the open- and closed-loop time history computer simulations performed for the same conditions.

Table 2 lists the finite element and experimental frequencies, open-loop damping, predicted closed-loop damping, and experimental closed-loop damping. The experimental and analytical frequencies for the first nine modes are fairly accurate, but at higher frequencies (not shown), this accuracy decreases considerably. The predicted and actual damping values achieved when implementing this controller are somewhat different. It is of interest to note that mode 2 showed no damping improvement in the experiment. This is due in part to the pendulum mode acceleration being nearly equal and opposite to the geometric change in acceleration due to gravity. Since the finite element model of the structure does not include nonlinear-gravity effects, the experimentally sensed acceleration for this mode is significantly lower than predicted. Although the damping obtained with the AVA controller is not predicted well, stability is conserved under modeling errors.

Conclusions

The implementation of an active vibration absorber has been experimentally demonstrated. Using only acceleration feedback, a second-order controller design is presented that represents an active tuned spring-mass-damper assembly. Experiment and simulation results show the controller performs well even in the presence of modeling errors. Since acceleration sensors are relatively inexpensive and provide an inertial measurement, this type of sensor is likely to be used in structural control applications. The controller design presented herein permits direct use of acceleration signals without the need for prefiltering. Moreover, the active vibration absorber has high stability robustness for collocated sensors and actuators as only its performance, not its stability, is model-based. General implementation issues are discussed to insure that the reader can properly use this technology in other applications. The effects of poor implementation are shown using experimental data. With proper implementation, the controller successfully augments the damping of the structure. This simple controller design, due to its high level of stability robustness, has great potential for distributed, inner- and outer-loop control systems for spacecraft structures.

References

[1]Benhabid, R. J., Flashner, H. K., and Tung, F. C., "ACOSS Fourteen (Active Control of Space Structures)," Rome Air Development Center, RADC-TR-83-51, Final Rept., Griffiss AFB, New York, March 1983.

[2]Irwin, R. D., Jones, V. L., Rice, S. A., Tollison, D. K., and Seltzer, S. M., "Active Control Technique Evaluation for Spacecraft (ACES)," Air Force Wright Aeronautical Labs., Final Rept., AFWAL-TR-88-3038, Wright-Patterson AFB, OH, Aug. 1986–July 1987.

[3]Tanner, S., Pappa, R., Sulla, J., Elliott, K., Miserentino, B., Bailey, J., Cooper, P., and Williams, B., "Mini-Mast CSI Testbed User's Guide," NASA TM-102630, Langley Research Center, Feb. 1991.

[4]Belvin, W. K., Elliott, K., Horta, L., Bailey, J., Bruner, A., Sulla, J., Wen, J., and Ugoletti, R., "Langley's CSI Evolutionary Model: Phase O," NASA TM-104165, Langley Research Center, Nov. 1991.

[5]Juang, J.-N., and Phan, M., "Robust Controller Designs for Second-Order Dynamic Systems: A Virtual Passive Approach," NASA TM-102666, NASA Langley Research Center, May 1990; also, *Journal of Guidance, Control, and Dynamics* (to be published).

[6]Snowdon, J. C., *Vibration and Shock in Damped Mechanical Systems,* Wiley, New York, 1968, Chap. 4.